Journal of Harbin Engineering University Vol 44 No. 7
ISSN: 1006-7043 July 2023

Investigation Of AA7075 MMC Reinforced By Al0.5cocragni Heap Through Stir Casting And Cryorolling

P. Thangavel*, K. M. Arunraja, S. Prakasam, P. Lingeswaran

Shree Venkateshwara Hi-Tech Engineering College, Gobichettipalayam, Erode-638455, Tamilnadu.

*Corresponding Author: thangspro@gmail.com *

Abstract

Stir casting, and subsequent rolling (room temperature rolling (RTR) and cryorolling (CR))employs to create AA7075 MMCs reinforced with Al0.5CoCrAgNi high entropy alloy particles (HEAp). The microstructures and mechanical characteristics of AA7075HEAp MMCs examine in this research. Stir-cast AA7075HEAp MMCs have an enhancement in ultimate tensile strength compared to AA7075, with the addition of HEAp (6 wt%). The mechanical characteristics of the cryo-rolling AA7075HEAp metal matrix compositeswere superior to those of the RTR-obtained MMCs. At increasing rolling deformation and lower HEAp mass percent, the discrepancies in mechanical characteristics between the CR and RTR-obtained AA7075HEAp MMCs widened. Scanning and transmission electron microscopy after RTR revealed multiple cavities in AA7075HEAp metal matrix composites, which were not present in cryo-rolling metal matrix composites. Researchers concluded that cryogenic temperatures change metal matrix composites' microvoids and mechanical characteristics.

Keywords: Mechanical properties, cryo-rolling, room temperature rolling, scanning electron microscope, Transmission electron microscope, aluminum.

1. Introduction

Metal matrix composites have gained popularity in recent years (MMCs). Aluminum matrix composites (AMC) consume the benefits of high toughness, reliability, and excellent abrasive resistance, making them an attractive option as lightweight materials continue to advance. Aerospace, transportation, and automotive industries have significantly used AMCs [1]. Presently, ceramic and metallic particles are primarily employed to reinforce AMCs[2]. Because of the increased interface bonding strength between the aluminum matrix and the metallic particle reinforcement, MMCs can benefit from adding metallic particles as reinforcement[3]. Similarly, a novel metallic substance, high-entropy alloy (HEA), has recently been incorporated into AMCs as reinforcement[4].

To increase the hardness and modulus of AA5052 metal matrix composites, the authors[5] used the vacuum hot-pressing sintering method to manufacture AA5052 MMCs reinforced with Al0.6CoCrAgNi HEAp. They used the spark plasma sintering technique, and the authors[6]created Al1.0CoCrAgNi HEAp-reinforced AMCs. Improvements in yield strength and elongation in AMCs as the temperature raised from 540 to 600°C. Researchers [7]used friction stir welding to create reinforcements for AA5083 MMCs made from Al0.8CoCrFeNi HEAp. When compared to the matrix, the composites exhibit increased hardness (by 56%), yield strength (42%), and ultimate tensile strength (22%), while the mean grain size of the AA5083HEAp metal matrix composites is condensed (47%)[8].

Cryogenic temperatures improve the strength and flexibility of aluminum alloys and certain HEAs compared to their room temperature values[9], [10]. Cryorolling (CR) produces ultrafine grain aluminum alloys and HEA strips. Substantial suppression of dynamic recovery observed during cryogenic deformation and dislocation accumulation, dislocation cells, and other microstructure formation were all the direct results [11]. Researchers[12]used the microstructure and mechanical characteristics of AA7075 using CR. Due to dynamic recovery preventions, CR significantly improved aluminum

alloy's tensile and yield strength. For their preparation of AA7075 sheets, the authors[13]used chemical vapor deposition, and they found that the material exhibited a higher density of dislocation cells than was previously reported. Ultrafine-grained sheets of AA1060 were obtained by CR and prepared by the authors[14]. To put it another way, the tensile strength(TS) of materials formed by cryo-rolling is 40% more than that of materials attained by RTR under the same deformation situation.

Table 1. Chemical arrangement of AA7075 (wt%).

Si	Fe	Cu	Mg	Zn	Mn	Cr	Al
0.08	0.24	1.5	2.4	5.8	0.06	0.2	Bal

Table 2. Chemical arrangement of Al0.5CoCrAgNi HEAps

Chromium	Silver	Nickel	Aluminum	Cobalt
23.31	24.21	25.36	5.93	Bal.

Medium-entropy alloy strips make via cryo-rolling, and the authors discovered that the process enhanced the alloy's mechanical characteristics[15], [16]. Recent years have also seen CR employed in the preparation of composite strips. According to the authors[17], CR can lessen the severity of edge cracks in the Aluminium/Titanium composite strips. Mechanical characteristics of Al/Cu composite strips generated by the CR method enhanced by literatures[18]–[20]. Products made from AMCs may have flaws due to the usual plastic deformation process because the elastic modulus of the strengthening is significantly variant from that of the AMC[21], [22]. Since CR has great cryogenic mechanical qualities, researchers want to employ it to fix this flaw. This study used stir-casting and subsequent rolling to create AA7075HEAp MMCs strips. Researchers looked at the microstructure and mechanical characteristics of room temperature rolling and cryo-rolling AA7075HEAp metal matrix composites. CR testing shows that the mechanical qualities of AA7075 HEAp strips are superior. We also go through how CR works to boost mechanical attributes.

2. Materials and methods

Manufacturing AA7075HEAp MMCs involved using commercial AA7075 ingot and Al0.5CoCrAgNi HEAp. Tables 1 and 2 detail the AA7075 and Al0.5CoCrAgNi HEAp's chemical arrangement. The particle size distribution of HEApindicates in Fig. 1. Stir casting is employed to create the AA7075HEAp MMCs. Stir casting depicts in Fig. 2 as a simplified diagram. The ingot of AA7075 was melted in a resistance furnace at a temperature of 1093 K. HEAp, wrapped in high-purity aluminum foil,and added to the molten alloy. The mixture was stirred mechanically for three minutes. The ingots make by pouring molten AA7075HEAp MMCs into a heated mold. Ingots of AA7075HEAp MMCs were made with HEAp mass fractions of 0%, 3%, 6% and 9%.

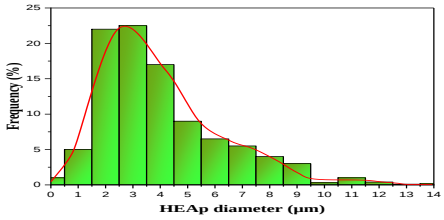

Fig. 1. Particles size distribution of HEap

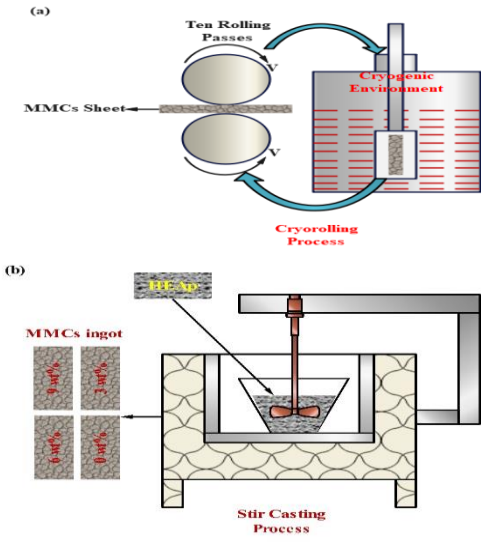

Fig. 2. Diagram of the AA7075–High Entropy alloy particles: (a) cryo-rolling progression and b) stir casting technique.

Table 3 AA7075-High Entropy alloy particles Rolling arrangement.

Rolling pass	1	2	3	4	5	6	7	8	9	10
The thickness of the specimen (mm)	1.82 ± 0.03	1.62 ± 0.03	1.42 ± 0.02	1.18 ± 0.02	1.02 ± 0.01	0.83 ± 0.01	0.59 ± 0.02	0.38 ± 0.01	0.26 ± 0.03	0.11 ± 0.01

Wire-cut electrical discharge machining utilizes to cut 2.00 mm thick sheets from AA7075HEAp MMCs ingots. After that, RTR and CR were used to process the sheets. There was a temperature difference of 197°C between the RTR and CR, or 299K and 78K, respectively. Table 3 details the rotating schedule. Microstructure and mechanical propertiesconduct on the rolled specimen with thicknesses of 1.02 mm,0.41mm, and 0.12mm rolling reduction ratiosof 40%,60%, and 80%, respectively.

The AA7075HEAp MMCs' microhardness was measured using a Vickers hardness tester. The tensile machine with a strain rate of $1x10^{-3}s^{-1}$employs for the tensile tests. The testing was perpendicular to the rolling direction, kept the materials in a similar condition, and repeated three times.

X-ray diffraction employs to evaluate the phase structures of the High entropy alloy particles and AA7075 HEAp MMCs. The microstructures and tensile fracture morphology of the AA7075 HEApsmetal matrix composites were analyzed using SEM. EDS performs to calculate the fundamental and phase dispersals of the AA7075 HEAps metal matrix composites. Electropolishing to smooth the samples for microscopic analysis. The researcher may get a high-quality finish with an electrolytic polishing power supply of 13-19 V, a density of 0.2-0.6A, and a polishing duration of the 30s. Transmission electron microscopy performs characterization of disruptions and other microstructural analysis in AA7075 HEAps metal matrix composites[23], [24]. After undergoing focused ion beam preparation, the samples were ready for transmission electron microscopy (TEM) analysis.

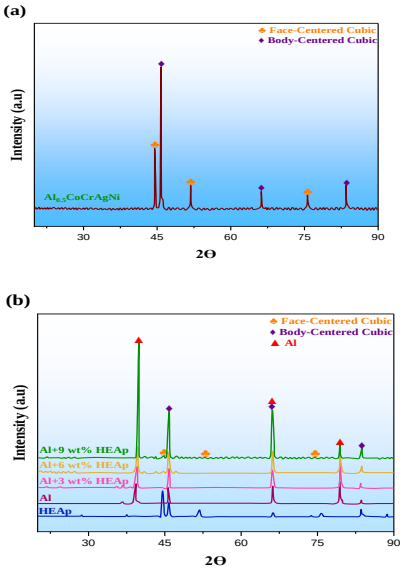

Fig. 3. XRD of (a) Al0.5CoCrAgNi and (b) AA7075 –HEAp MMCs with variant HEAp percentage.

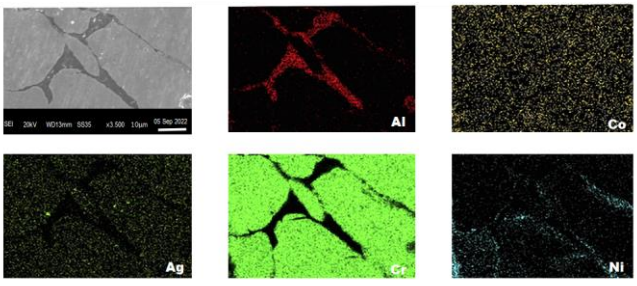

Fig. 4. Scanning electron microscopic images and element distribution of high entropy alloy particles in as-cast AA7075–9 wt% HEAps metal matrix composites.

3. Results

3.1. XRD analysis of HEApsand AA7075–HEAps metal matrix composites

The X-ray Diffraction spectrum of the Al0.5CoCrAgNi high entropy alloy particles and the AA7075HEAp metal matrix compositesindicates in Figure. 3. Fig. 3a shows that the Al0.5CoCrAgNi HEAp has a two-phase structure consisting of face-centered cubic (FCC) and body-centered cubic (BCC). The BCC structure's diffraction peaks observe in the (110), (200), and (211) directions. When x is between 0.3 and 0.8, the authors[25]found that Al0.5CoCrAgNi HEA has two-phase structures that consist of FCC and BCC. In addition, the authors[26]noted that Al0.5CoCrAgNi high entropy alloy is a distinctive two-phase-structural alloy with high toughness and high ductileness. Figure 3b displays the XRD outcomes for varying HEAp mass fractions added to the AA7075 matrix. The XRD spectrum of the AA7075HEAp MMCs showed the presence of HEAp, demonstrating that they introduce into the AA7075 matrix the uniquecrystal plane of the Al0.5CoCrAgNi HEA. The BCC phase's diffraction peak strength grew progressively with increasing HEAp mass fraction, whereas this trend was absent in HEAp-free AA7075.

3.2. Microstructural analysis of AA7075–HEAp metal matrix composites.

Figure 4 depicts a scanning electron micrograph image of the High entropy alloy particles in as-cast AA7075HEAp Metal matrix composites and the surface scanning outcomes for the same region. Aluminum, Cobalt, Silver, Chromium, and Nickel were the five components that made up the HEAp. Scanning results for the surface indicates in Fig. 4, where the five elements mentioned above show in their respective distributions.

SEM pictures of AA7075 HEAp MMCs with varying degrees of rolling deformation indicates in Fig. 5. RTR and CR have performed with 40% and 80% reduction ratios, respectively (see Fig. 5a–d). There are several microvoids in the AA7075HEAp MMCs as a result of RTR. The microvoids significantly increased as deformation went from 40% to 80%. The low CR temperature stifled dynamic recovery during rolling and led to a more consistent material structure.

Similarly, the authors[27], [28] research on the topic in a cryogenic setting confirmed this unique phenomenon. Additionally, as seen in Fig. 5a and c, although the rolling reduction of the Room Temperature Rolling and Cryo-rolling were similar, their distorted microstructural characteristics were markedly dissimilar, indicating that the two materials were not interchangeable[29]. Since the CR, the HEAp's reinforcement phase has been more consistent and prolonged than it was after the RTR.

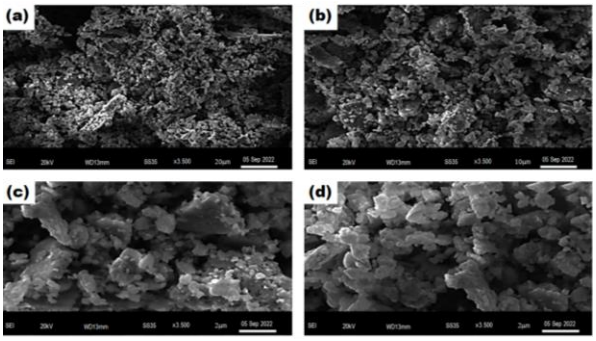

Fig. 5. Scanning electron microscopic images of AA7075–6 wt% HEAp metal matrix: room temperature rolling with reduction of (a) 40% (b) 80%; cryo-rolling with reduction of (c) 40% (d) 80%.

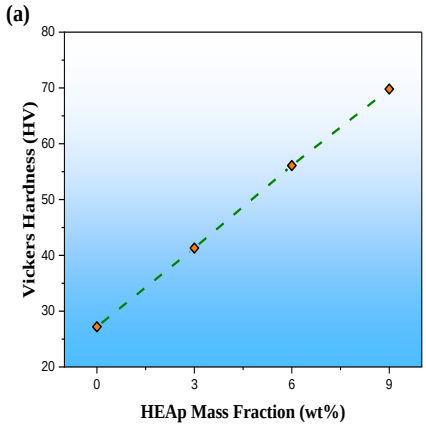

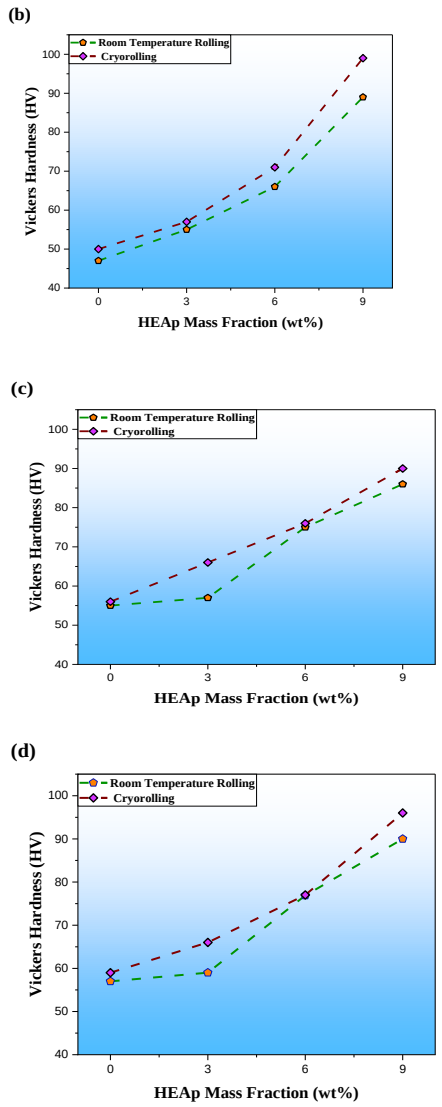

Fig. 6. (a) AA7075 –HEAp MMCs; rolled AA7075 –HEApmetal matrix composites at a reduced proportion of (b) 40%, (c) 60%, and (d) 80%Vickers hardness .

3.3. Mechanical characteristics of AA7075–HEAp metal matrix composites.

The microhardness range of cast and rolled AA7075 HEAp MMCs shown in Fig. 6. Figure 6a demonstrates that the inclusion of HEAp significantly increased the toughness of the AA7075 HEAp MMCs. Incorporating four distinct types of HEAp resulted in microhardness ranges of 27.2, 41.3, 56.1, and 69.8 HV. After totaling 9wt% high entropy alloy particles, the microhardness ranges of the AA7075 HEAp MMCs rise by 164.2 percent. Microhardness runs for the AA7075 HEAp metal matrix compositesare attained via room temperature rolling and cryo-rolling at varying degrees of deformation, asshown in Fig. 6b-d. The CR AA7075 HEAp MMCs have more microhardness than the RTR. The AA7075 HEAp MMCs showed more microhardness value rise than the AA7075 under identical deformation conditions. The ultimate tensile strength, shown in Fig. 7, corroborated these findings.

Figure 7 depicts the transitional tensile mechanical characteristics of AA7075 HEAp MMCs. With a rise in HEAp, the as-cast mechanical characteristics of AA7075 MMCs may have improved. As for AA7075's ultimate tensile strength, it measured in at 75.1MPa. Adding 6% HEAp increased the AA7075 MMCs' ultimate tensile strength to 118MPa. Simultaneously, the elongation reached 33.2%. However, the ultimate tensile strength is slightly improved when the HEAp mass fraction improves to 9wt%. The Vickers hardness measurements agree with this. Figure 7a–d demonstrates that following CR, all mechanical properties of the materials enhance compared to RTR. The CR AA7075 6 wt percent HEAp MMCs in Fig. 7c had an ultimate tensile strength of 195 MPa and an elongation of 16.4 percent at 40% deformation, while the RTR MMCs had values of 171MPa and 12.2%, respectively. The elongation of the Cryo-rollingmetal matrix composites was 34.2% greater than that of the Room temperature rollingmetal matrix composites, and their ultimate tensile strength was 16.1% greater. Mechanical property variations between RTR and CR samples were also minimal when HEAp constituted a minor percentage of the total mass[30]. The enhancement of the CR samples' mechanical characteristics was especially noticeable once the mass fraction of high entropy alloy particles raised to 3 wt %. For rolled MMCs, the addition of 9 wt % HEAp resulted in generally poorer mechanical characteristics than AA7075-6wt %HEAp metal matrix composites.

3.4. AA7075–HEAp MMCs Fracture surface

Tensile fracture morphology of the AA7075 -9% HEAp metal matrix composites following room temperature rolling and cryo-rollingindicates in

Fig. 8. Composites' elongation is strongly linked to fracture morphology [31]. As the rolling distortion increased, the number of dimples in the crack dropped dramatically. Additionally, the size and depth of the dimples shrank, and the torn edges of the dimples were visible[32]. It conformed to the rule that the AA7075HEAp MMCs' elongation decreased as deformation increased. The mechanical properties showed that the CR AA7075HEAp MMCs had superior elongation properties to the RTR MMCs. Figure 8a and d display that the CR MMCs had a much higher dimple count than the RTR MMCs. This microstructural difference accounted for finding CR MMCs extended further than RTR MMCs. A high no. of tearing limits and quasi- cleavage crackstructures emerged in the room temperature rolling metal matrix composites, shown in Fig. 8c and f. Though, the quantity and thicknesses of the tear edges in the cryo-rollingmetal matrix composites were far lower than those of the room temperature rolling metal matrix composites, further demonstrating the elongation of the cryo-rollingmetal matrix compositeswas superior[33]. One interesting finding was that the HEAp broke off at the tensile fracture in the room temperature rolling metal matrix composites. The high entropy alloy particles and AA7075 matrix in the cryo-rollingmetal matrix compositesdisplay superior bonding capacity and resist peeling.

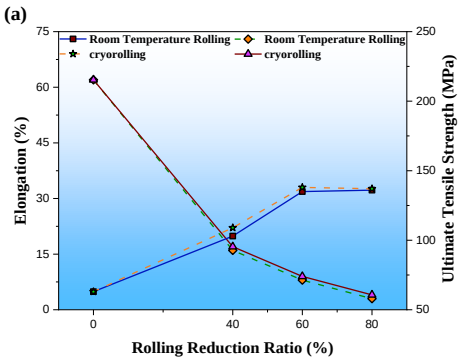

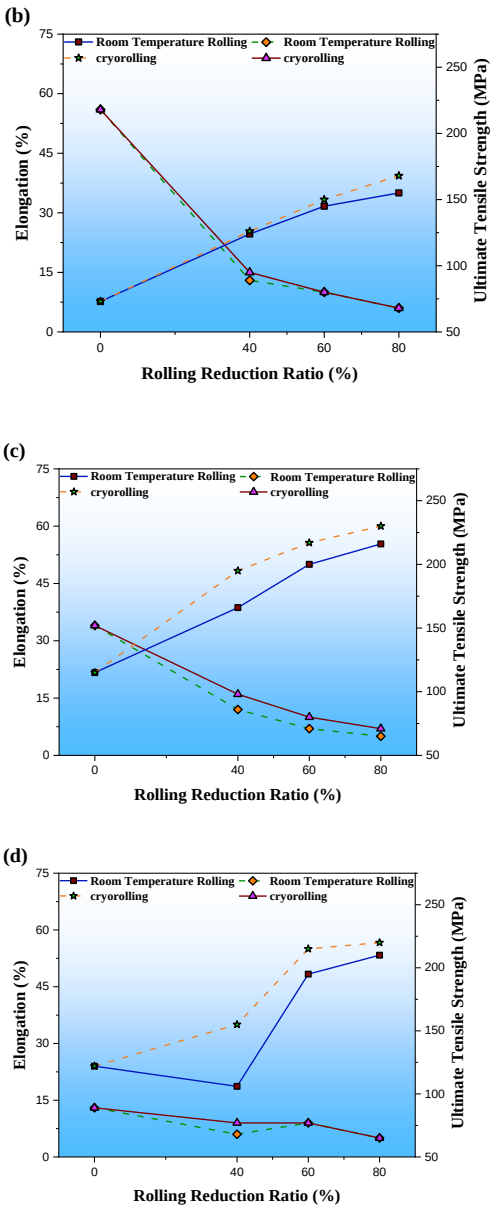

Fig. 7. Ultimate Tensile Strength and Elongation of AA7075 –high entropy alloy particles metal matrix composites at 299K, 78 K (a) AA7075 and AA7075 with (b) 3 wt% (c)

6(d) 9wt% of high entropy alloy particles.

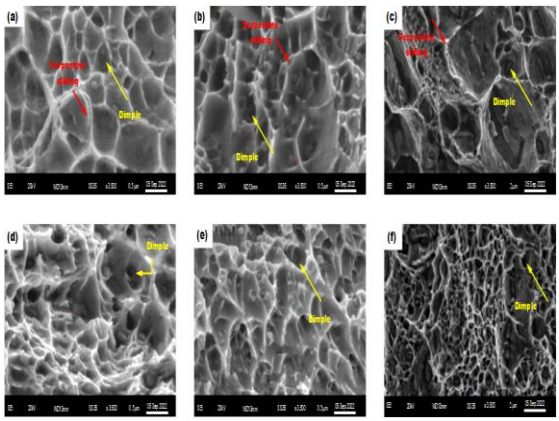

Fig. 8. Fracture morphology of AA7075 – 6 wt% high entropy alloy nanoparticles: Room temperature rolling with reducedproportion of (a) 40%, (b) 60%, (c) 80%; cryo-rolling with reducedproportion of (d) 40%, (e) 60%, (f) 80%.

4. Discussions

4.1. Impact of cryogenic deformation on fracture morphology and microvoid in metal matrix composites

Figure 8 shows that the RTR MMCs, and CR MMCs, experienced HEAp coming off during tensile fracture. Meanwhile, Fig. 5 indicates more flaws in the RTR MMCs compared to the CR MMCs. The AA7075HEAp MMCs underwent volume contraction at the CR temperature of 78 K, formulated:

$$V_T = V_0 e^{\alpha(T-T_0)} \qquad (1)$$

whereα is the thermal expansion coefficient. When moving from a temperature of,$T_0$to T, the associated volume shifts from,V_o to V_T. The above calculation demonstrates the dramatic effect of a temperature shift on a solid's volume. When cryorolling (CR) perform at a temperature of 78 K, a substantial temperature differential (221K) causes a significant volume shrinking impact. The author [34]described thatvolume shrinkage significantly altered materials' microstructures and mechanical characteristics. Both the aluminum alloy matrix and HEAp undergo volume reduction during CR. Since the thermal coefficient of the AA7075 matrix was more significant than that of the HEAp matrix $(68.1 \times 10^{-6}\mathrm{K}^{-1})$Vs.$(11.8 \times 10^{-6}\mathrm{K}^{-1})$, the degrees of volume shrinkage for the two matrices were distinct.

Since aluminum alloy undergoes a more significant volume shrinkage than other metals, the alloy's matrix forms a stronger bond with the HEAp. The HEAp will be less prone to separate with better adhesion during a tensile fracture. The HEAp is less stable when the RTR lacks this effect, increasing the likelihood that it may detach from the aluminum alloy matrix. Figures 9(a, b) also show that fracture was discovered close to high entropy alloy particles in the Room Temperature Rolling metal matrix composites. The volume shrinking effect of CR allowed for avoiding these flaws, leading to improved mechanical characteristics. Fractures and other faults are not visible in CR, as seen in Figures 9c and 9d. The SEM findings depicted in Fig. 5a-b and c-d corroborate the presence of this microstructural flaw.

Furthermore, cryogenic environments enhance the flexibility of Al alloys and HEA compared to ambient environments [35], [36]. A possible factor in the MMC strips' flawless quality after CR is their improved deformation performance in the cold.

4.2. Impactof mechanical properties of Metal matrix composites on cryogenic deformation

The cryogenic situation has significant dislocations [37] and substructures [38]. Since the atomic energy is less during cryogenic deformation, dynamic recovery is significantly impeded [39]. As the dislocations continue to amass and entangle, a cellular structure begins to take shape. Displacement cells generated by more density displacement tangles are visible in CR materials, as shown in Fig. 9c. Figure 9d shows that as the deformation of CR rises, sub-crystalline structures form as a result of the exceptionally high dislocation density. Improved global mechanical characteristics in AA7075HEAp MMCs attributed to high densities of dislocations and substructures[40], [41].

It hypothesized that materials exposed to cryogenic settings obtain a great deal of stored

energy with high-density dislocations, enabling the rolling of polished grains [42]. Figure 10 represents the statistical data on the effect of rolling distortion on the grain size of AA7075 HEAp MMCs. Figure. 10a-b and c-d illustrate the considerable variation in grain size between room temperature rolling and Cryo-rolling-produced AA7075 HEAp metal matrix composites, even when the rolling deformation setting is constant. At 40% rolling deformation, RTR produces AA7075 HEAp MMCs with a grain size of 594 nm, while CR produces AA7075 HEAp MMCs with a grain size of 342 nm. Standard grain size has shrunk by 43.2%. Grain refinement is noticeable in the CR-obtained AA7075 HEAp MMCs. The Hall–Petch formula indicates that a more refined grain size results in greater material strength. Since CR MMCs have a far smaller grain size than RTR, they are much more powerful.

Figures 5 and 9 show that the elongation of cryo-rollingmetal matrix composite strips is greater than that of RTR MMCs because there are fewer faults in the former. A further consequence of volume contraction is an increase in the material's internal stress, which causes dislocations. The resistance to dislocation movement increases when a displacement contacts another disruption on the slip plane during dislocation movement, as predicted by dislocation strengthening theory [43]–[45]. Since this strengthens the material, volume shrinking is beneficial.

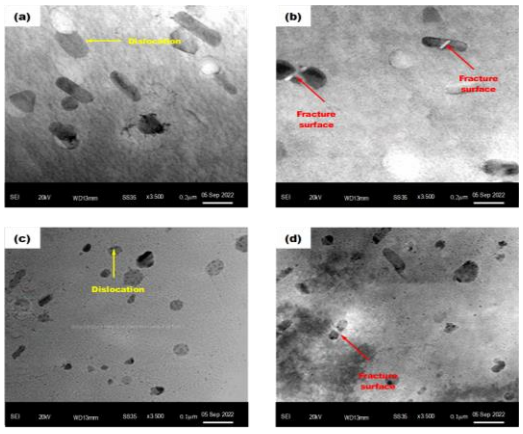

Fig. 9. Transmission Electron microscopic images of the room temperature rolling AA7075 – 9 wt% HEAps metal matrix composites at (a) 40% and (b) 80% deformation and the cryo-rolling AA7075 – 9 wt% HEAps metal matrix composites at (c) 40% and (d) 80% deformation.

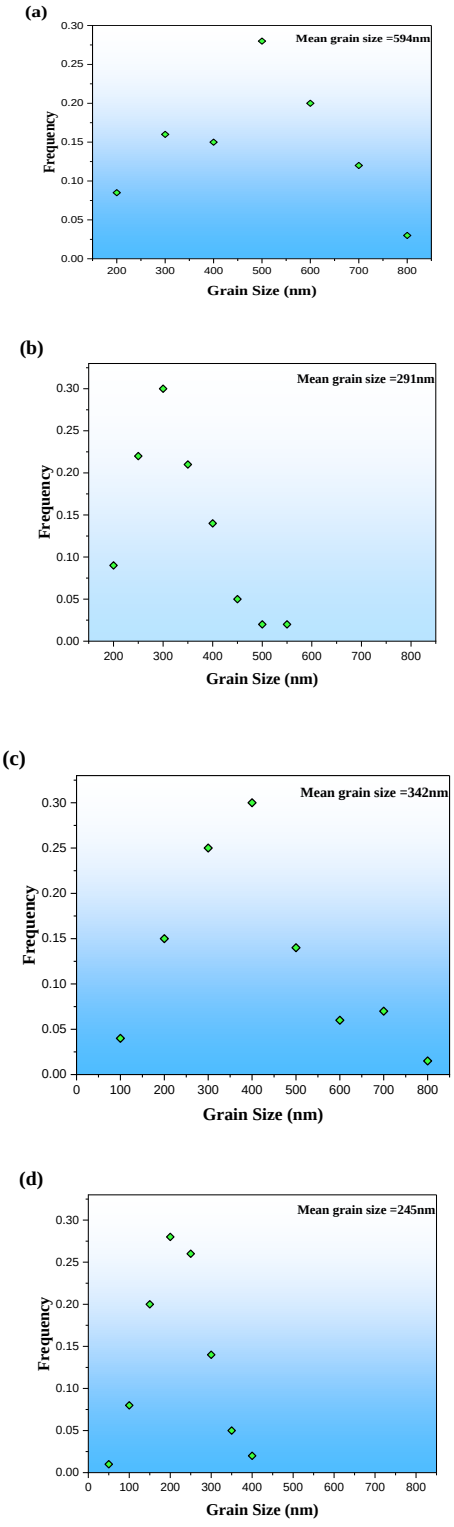

Fig. 10. Grain size at room temperature rolling AA7075 – 9 wt% HEAps metal matrix composites with a reduced proportion of (a) 40% (b) 80%; cryo-rolling AA7075 – 9 wt% HEAps metal matrix composites with rolling reduced proportion of (c) 40% (d) 80%.

5. Conclusions

(1) Compared to MMCs obtained by RTR, AA7075HEAp MMCs received using CR have fewer flaws. During tensile fracture, the HEAp in the cryo-rolling AA7075 HEAp metal matrix composites did not detach from the AA7075 matrix as it did in the RTR.

(2) The as-cast AA7075HEAp MMCs had an ultimate tensile strength of 118 MPa, an increase of 75.1% compared to that with no extra HEAp, and an elongation of 33.2%.

(3) Compared to RTR, CR AA7075HEAp MMCs exhibited superior mechanical characteristics. At 40% deformation, the CR AA70756 wt percent HEAp MMCs had strength and elongation that were 16.1 and 34.2% more excellent, respectively, than RTR.

(4) The CR can potentially increase the mechanical characteristics of AA7075- HEAp MMCs during deformation. It also has the advantage of reducing defects in these materials relative to RTR, making it a novel strategy for creating high-performance MMCs free of defects.

References

[1] S. Venkatesan and M. Ramu, “Effect of mechanical properties and corrosion behavior of sputtered Ti thin film on AA7075 substrate,” *High Temp. - High Press.*, vol. 46, no. 2, pp. 115–131, 2017, [Online]. Available: https://www.scopus.com/inward/record.uri?eid=2-s2.0-85016552786&partnerID=40&md5=e1159db1c4de937cc431373e95f1448d

[2] Z. He, N. Jia, H. Wang, H. Yan, and Y. Shen, “Synergy effect of multi-strengthening mechanisms in FeMnCoCrN HEA at cryogenic temperature,” *J. Mater. Sci. Technol.*, vol. 86, pp. 158–170, 2021, doi: 10.1016/j.jmst.2020.12.079.

[3] T. P. Tejasvi, H. M. Somashekar, and V. Ranjith, “Experimental Investigations on Microstructure and Mechanical Properties of Retrogression and Reaging (RRA)-Treated AA7075 (Al-Zn-Mg) Alloy,” *J. Inst. Eng. Ser. D*, vol. 103, no. 1, pp. 161–171, 2022, doi: 10.1007/s40033-021-00326-6.

[4] K. Ozturk, R. Gecu, and A. Karaaslan, “Preform-Based Production of Al2O3-Reinforced Aluminium Matrix Composites by Using Various Modification Techniques,” *Met. Mater. Int.*, vol. 27, no. 5, pp. 1327–1336, 2021, doi: 10.1007/s12540-019-00520-y.

[5] C. Wang, X. Lin, L. Wang, S. Zhang, and W. Huang, “Cryogenic mechanical properties of 316L stainless steel fabricated by selective laser melting,” *Mater. Sci. Eng. A*, vol. 815, 2021, doi: 10.1016/j.msea.2021.141317.

[6] G. He, K. Li, Y. Yang, Y. Liu, W. Wu, and C. Huang, “Effect of heat treatment on the microstructure and mechanical properties of cryogenic rolling 2195 Al–Cu–Li alloy,” *Mater. Sci. Eng. A*, vol. 822, 2021, doi: 10.1016/j.msea.2021.141682.

[7] H. Rak Song and W. J. Nam, “Effects of annealing temperature and time on the microstructural evolution and corresponding mechanical properties of 5083 Al alloy deformed at cryogenic and room temperatures,” *Int. J. Mater. Res.*, vol. 96, no. 3, pp. 276–280, 2022, doi: 10.3139/ijmr-2005-0049.

[8] T. Sunar, T. Tuncay, D. Özyürek, and M. Gürü, “Investigation of Mechanical Properties of AA7075 Alloys Aged by Various Heat Treatments,” *Phys. Met. Metallogr.*, vol. 121, no. 14, pp. 1440–1446, 2020, doi: 10.1134/S0031918X20140161.

[9] J. Huang *et al.*, “Effects of Cryogenic Deformation on Second-Phase Al2Cu Particles and Mechanical Properties of 2219 Al–Cu Alloy Rings,” *Met. Mater. Int.*, vol. 27, no. 5, pp. 815–824, 2021, doi: 10.1007/s12540-019-00468-z.

[10] S. Fritsch and M. F.-X. Wagner, “On the effect of natural aging prior to low temperature ECAP of a high-strength aluminum alloy,” *Metals (Basel).*, vol. 8, no. 1, 2018, doi: 10.3390/met8010063.

[11] H. M. Enginsoy, F. Gatamorta, E. Bayraktar,

M. H. Robert, and I. Miskioglu, "Experimental and numerical study of Al-Nb 2 Al composites via associated procedure of powder metallurgy and thixoforming," *Compos. Part B Eng.*, vol. 162, pp. 397–410, 2019, doi: 10.1016/j.compositesb.2018.12.138.

[12] M. Velusamy, S. P. Kumarasa, and S. K. Sathiavelu, "Investigation of Electrical Discharge Machining Properties of Reinforced Cryogenic Treated AA7075 Composites," *Chiang Mai J. Sci.*, vol. 49, no. 4, pp. 1184–1204, 2022, doi: 10.12982/CMJS.2022.065.

[13] B. Feng, B. Gu, and S. Li, "Cryogenic deformation behavior and failure mechanism of AA7075 alloy sheets tempered at different conditions," *Mater. Sci. Eng. A*, vol. 848, 2022, doi: 10.1016/j.msea.2022.143396.

[14] J. W. Won *et al.*, "High strength and ductility of pure titanium via twin-structure control using cryogenic deformation," *Scr. Mater.*, vol. 178, pp. 94–98, 2020, doi: 10.1016/j.scriptamat.2019.11.009.

[15] F. Dong, Y. Yi, C. Huang, and S. Huang, "Influence of cryogenic deformation on second-phase particles, grain structure, and mechanical properties of Al–Cu–Mn alloy," *J. Alloys Compd.*, vol. 827, 2020, doi: 10.1016/j.jallcom.2020.154300.

[16] Y. Wu, J. Liu, L. Bhatta, C. Kong, and H. Yu, "Study of texture analysis on asymmetric cryorolled and annealed cocrni medium entropy alloy," *Crystals*, vol. 10, no. 12, pp. 1–12, 2020, doi: 10.3390/cryst10121154.

[17] K. Gopala Krishna, G. Das, K. Venkateswarlu, and K. C. Hari Kumar, "Studies on Aging and Corrosion Properties of Cryorolled Al–Zn–Mg–Cu (AA7075) Alloy," *Trans. Indian Inst. Met.*, vol. 70, no. 3, pp. 817–825, 2017, doi: 10.1007/s12666-017-1064-3.

[18] H. Gu *et al.*, "Enhanced Mechanical Properties of AA5083 Matrix Composite via Introducing Al0.5CoCrFeNi Particles and Cryorolling," *Acta Metall. Sin. (English Lett.*, vol. 35, no. 6, pp. 879–889, 2022, doi: 10.1007/s40195-021-01351-w.

[19] K. S. Tun and M. Gupta, "Enhanced tensile properties and reversal of tension-compression asymmetry of magnesium reinforced with high entropy alloy particles," *Mater. Perform. Charact.*, vol. 8, no. 1, pp. 437–447, 2019, doi: 10.1520/MPC20190062.

[20] Z. Yuan *et al.*, "Effect of heat treatment on the interface of high-entropy alloy particles reinforced aluminum matrix composites," *J. Alloys Compd.*, vol. 822, 2020, doi: 10.1016/j.jallcom.2020.153658.

[21] Y. Chen, R. Wei, Q. Shao, and Z. Ji, "AZ91D Matrix Composites Reinforced with AlCrFeCoNi High-Entropy Alloy Particles Fabricated via Squeeze Casting," *Trans. Indian Inst. Met.*, 2022, doi: 10.1007/s12666-022-02652-z.

[22] M. Bahrami, M. K. Besharati Givi, K. Dehghani, and N. Parvin, "On the role of pin geometry in microstructure and mechanical properties of AA7075/SiC nano-composite fabricated by friction stir welding technique," *Mater. Des.*, vol. 53, pp. 519–527, 2014, doi: 10.1016/j.matdes.2013.07.049.

[23] D. Wang, S. Huang, Y. Yi, H. He, and C. Li, "Effects of cryogenic deformation on the microstructure and mechanical properties of high-strength aluminum alloys," *Mater. Charact.*, vol. 187, 2022, doi: 10.1016/j.matchar.2022.111831.

[24] B. Gruber *et al.*, "Mechanism of low temperature deformation in aluminium alloys," *Mater. Sci. Eng. A*, vol. 795, 2020, doi: 10.1016/j.msea.2020.139935.

[25] Y. Chen, Z. Ji, M. Hu, H. Xu, and G. Feng, "Microstructure and mechanical properties of AlCrFeCoNi high-entropy alloy particle reinforced Mg-9Al-1Zn matrix composites," *Int. J. Mater. Res.*, vol. 112, no. 7, pp. 538–545, 2021, doi: 10.1515/ijmr-2020-7953.

[26] K. Luo *et al.*, "AA1050 metal matrix composites reinforced by high-entropy alloy particles via stir casting and subsequent rolling," *J. Alloys Compd.*, vol. 893, 2022, doi: 10.1016/j.jallcom.2021.162370.

[27] F. A. Liyakath Ali, A. Soundarajan, D. R. Kanagaraj, G. Niranjan, and S. Ranganathan, "Unraveling the Mechanical Behavior of AA 7075 - WC Nanocomposites Developed through FSP Route," *SAE Tech. Pap.*, no. 2020, 2020, doi: 10.4271/2020-28-0404.

[28] S. V Alagarsamy and M. Ravichandran, "Synthesis, microstructure and properties of TiO2 reinforced AA7075 matrix composites via stir

casting route," *Mater. Res. Express*, vol. 6, no. 8, 2019, doi: 10.1088/2053-1591/ab1d3b.

[29] Y.-G. Hao and W. Liu, "Analysis on exceptional cryogenic mechanical properties of AA2219 alloy FSW joints in multi-scale," *Mater. Sci. Eng. A*, vol. 850, 2022, doi: 10.1016/j.msea.2022.143489.

[30] T. Lu *et al.*, "Exceptional strength-ductility combination of additively manufactured high-entropy alloy matrix composites reinforced with TiC nanoparticles at room and cryogenic temperatures," *Addit. Manuf.*, vol. 56, 2022, doi: 10.1016/j.addma.2022.102918.

[31] H. M. A. Mahmoud *et al.*, "Investigation of Mechanical Behavior and Microstructure Analysis of AA7075/SiC/B4C-Based Aluminium Hybrid Composites," *Adv. Mater. Sci. Eng.*, vol. 2022, 2022, doi: 10.1155/2022/2411848.

[32] K. Ozturk, R. Gecu, and A. Karaaslan, "Microstructure, wear and corrosion characteristics of multiple-reinforced (SiC–B4C–Al2O3) Al matrix composites produced by liquid metal infiltration," *Ceram. Int.*, vol. 47, no. 13, pp. 18274–18285, 2021, doi: 10.1016/j.ceramint.2021.03.147.

[33] P. Vishwakarma, S. Soni, and P. M. Mishra, "Effect of reinforcement and volume fraction on mechanical behaviour of AA7075/B4C/Fly-ash MMCp," *Int. J. Eng. Adv. Technol.*, vol. 8, no. 4, pp. 1503–1510, 2019, [Online]. Available: https://www.scopus.com/inward/record.uri?eid=2-s2.0-85067942840&partnerID=40&md5=e1ba508f756c50499f204fab6f22aec8

[34] K. Luo, Y. Wu, Y. Zhang, G. Lei, and H. Yu, "Study on Mechanical Properties and Microstructure of FeCoCrNi/Al Composites via Cryorolling," *Metals (Basel).*, vol. 12, no. 4, 2022, doi: 10.3390/met12040625.

[35] Y. Liu, J. Chen, X. Wang, T. Guo, and J. Liu, "Significantly improving strength and plasticity of Al-based composites by in-situ formed AlCoCrFeNi core–shell structure," *J. Mater. Res. Technol.*, vol. 15, pp. 4117–4129, 2021, doi: 10.1016/j.jmrt.2021.10.016.

[36] X. Yang *et al.*, "AlCoCrFeNi high-entropy alloy particle reinforced 5083Al matrix composites with fine grain structure fabricated by submerged friction stir processing," *J. Alloys Compd.*, vol. 836, 2020, doi: 10.1016/j.jallcom.2020.155411.

[37] K. Luo, S. Liu, H. Xiong, Y. Zhang, C. Kong, and H. Yu, "Mechanical Properties and Strengthening Mechanism of Aluminum Matrix Composites Reinforced by High-entropy Alloy Particles," *Met. Mater. Int.*, 2022, doi: 10.1007/s12540-021-01159-4.

[38] K. S. Tun and M. Gupta, "Enhanced mechanical properties and near unity yield asymmetry in equiatomic high entropy alloy particles reinforced magnesium composites," *J. Alloys Compd.*, vol. 810, 2019, doi: 10.1016/j.jallcom.2019.151909.

[39] Y. Zhang *et al.*, "Insight of high-entropy alloy particles-reinforced 2219 Al matrix composites via the ultrasonic casting technology," *Mater. Charact.*, vol. 182, 2021, doi: 10.1016/j.matchar.2021.111548.

[40] R. J. Golden Renjith Nimal, M. Chenthil, P. Gnaneswar, S. Veerendranath, and B. Ganesah Reddy, "Metallurgical and microstructural analysis on diffusion bonding of mg/al alloys using aluminium coating interlayer," *Int. J. Recent Technol. Eng.*, vol. 7, no. 6, pp. 631–633, 2019, [Online]. Available: https://www.scopus.com/inward/record.uri?eid=2-s2.0-85067083285&partnerID=40&md5=8d67496d0109685c20e6509239fedeef

[41] S. Chinnaiyan, S. Karuppazhagi, A. Veeramani, and S. Shanmugam, "Synthesis and forming behaviour of AA7075-TiC powder-metallurgy composites," *Mater. Tehnol.*, vol. 52, no. 6, pp. 809–812, 2018, doi: 10.17222/mit.2017.189.

[42] E. Radhakrishnan, L. A. Kumaraswamidhas, K. Palanikumar, and D. Muruganandam, "Strength and hardness studies of C44300 tube to AA7075-T651 tube plate threaded and unthreaded dissimilar joints fabricated by friction welding process," *J. Mater. Res. Technol.*, vol. 8, no. 4, pp. 3424–3433, 2019, doi: 10.1016/j.jmrt.2019.06.008.

[43] G. Manohar, K. M. Pandey, and S. R. Maity, "Effect of microwave sintering on the microstructure and mechanical properties of AA7075/B4C/ZrC hybrid nano composite fabricated by powder metallurgy techniques,"

Ceram. Int., vol. 47, no. 23, pp. 32610–32618, 2021, doi: 10.1016/j.ceramint.2021.08.156.
[44] G. Manohar, S. R. Maity, and K. M. Pandey, "Microstructural and Mechanical Properties of Microwave Sintered AA7075/Graphite/SiC Hybrid Composite Fabricated by Powder Metallurgy Techniques," *Silicon*, vol. 14, no. 10, pp. 5179–5189, 2022, doi: 10.1007/s12633-021-01299-7.
[45] K. L. Kishore and K. T. B. Padal, "Effect of graphene nano plateletson microstructural and wearbehavior of AA7075/Al2O3Nano composites," *Mater. Today Proc.*, vol. 62, pp. 4424–4431, 2022, doi: 10.1016/j.matpr.2022.04.903.